This is the accepted manuscript made available via CHORUS. The article has been published as:

Statistics of Dislocation Slip Avalanches in Nanosized Single Crystals Show Tuned Critical Behavior Predicted by a Simple Mean Field Model

Nir Friedman, Andrew T. Jennings, Georgios Tsekenis, Ju-Young Kim, Molei Tao, Jonathan T. Uhl, Julia R. Greer, and Karin A. Dahmen

Phys. Rev. Lett. **109**, 095507 — Published 30 August 2012

DOI: 10.1103/PhysRevLett.109.095507

Statistics of dislocation slip-avalanches in nano-sized single crystals show *tuned* critical behavior predicted by a simple mean field model.

Nir Friedman[1], Andrew T. Jennings[2], Georgios Tsekenis[1], Ju-Young Kim[3], Molei Tao[4], Jonathan T. Uhl, Julia R. Greer[2,5], and Karin A. Dahmen[1,]*

[1]Department of Physics, University of Illinois at Urbana-Champaign, 1110 West Green Street, Urbana, Illinois 61801-3080,
[2]Division of Engineering and Applied Sciences, MC309-81, Caltech, Pasadena, CA 91125-8100,
[3]School of Mechanical and Advanced Materials Engineering, Ulsan National Institute of Science and Technology (UNIST), Ulsan 689-798, Republic of Korea,
[4]Department of Computing and Mathematical Sciences, MC305-16, Caltech, Pasadena, CA91125-8100
[5]The Kavli Nanoscience Institute at the California Institute of Technology.

[*]To whom correspondence should be addressed. E-mail: dahmen@illinois.edu

We show that slowly sheared metallic nano-crystals deform via discrete strain-bursts (slips), whose size-distributions follow power-laws *with stress-dependent cutoffs*. We show for the first time that plasticity reflects *tuned* criticality, by collapsing the stress-dependent slip-size distributions onto a predicted scaling-*function*. Both, power-law exponents and scaling-function agree with mean-field theory predictions. Our study of 7 materials, 2 crystal structures, at various deformation-rates, stresses, and crystal sizes down to 75 nm, attests to the universal characteristics of plasticity.

PACS : 62.25.-g, 61.72.Lk, 61.82.Bg, 89.75.Da, 64.70.qj

Introduction:

Sheared small-scale crystals deform via a sequence of discrete slips, measurable either as steps in stress-strain curves or as acoustic emission pulses [1-13]. We show that the statistical distributions of the slip-sizes, and their stress-dependence (1) reflect *tuned* criticality, (2) agree with the predictions of a simple mean field theory (MFT) model, down to 75 nm diameter samples, and (3) reflect the same scaling behavior (universality) for a wide variety of materials, crystal structures, size-scales, and experimental parameters.

The slips are caused by dislocation slip-avalanches resulting from rapid dislocation nucleation or sudden releases of dislocations from pinned sources. They stop when all

slipping dislocation segments have either repinned or are annihilated. Recent experiments on the axial compression of micron and sub-micron sized crystals reported that the stress-integrated distributions (histograms) $D_{int}(S)$ of all slip-sizes S (starting from the initiation of compression to pillar failure), follow a power-law $D_{int}(S) \sim S^{-1.5}$ over several decades in S. Here S is the total axial displacement during an avalanche (see Supplementary Online Material (SOM)). This has been seen in experiments on micron and sub-micron pillars of face-centered cubic (fcc) metals (Cu, Al, Au, Ni), and one body-centered cubic (bcc) metal (Mo) [8,9,14-16]. However, up to now, the slip statistics were far from understood. Here we report three main results that provide a new unified understanding:

(1) Tuned criticality: Previous experimental studies focused on fitting exponents κ to power-law distributions $D(S) \sim S^{-\kappa}$, similar to self-organized criticality (SOC) [5,6,8]. SOC assumes that the ("cutoff-") size S_{max} of the largest observed avalanche exclusively depends on the system-size, and not on other experimental parameters. However, a simple analytical MFT model [2] and simulations [1] predict that the cutoff S_{max} can also depend on the stress, implying that plasticity reflects *tuned* criticality. The long-standing fundamental debate of SOC versus tuned criticality so far has remained unresolved for plasticity, due to a lack of experimental evidence of cutoff-tuneability. Here we show for the first time that for nano-crystals the cutoff-size grows as the stress approaches the failure-stress, (or "critical stress") τ_c as predicted by MFT and simulations [1,2]. Below the critical stress, a slow stress-increase in the material produces microscopically small slip-avalanches. Above the critical stress τ_c the material deforms in a macroscopic slip-avalanche until it fails. The model predicts that the critical stress τ_c is a critical point separating these two regimes. (The value of τ_c depends on the details of the system [17-19].) Near τ_c the system shows *universal* (detail-independent) avalanche statistics, as predicted by the theory of phase transitions and the renormalization group [2,18,19]. We extract a predicted scaling-collapse of the stress-dependent avalanche-size distributions from the experiments which shows that plasticity indeed reflects the predicted tuned critical point with stress as a tuning-parameter. We also show why tuned criticality was not observed before in experiments and how it is reconciled with previous experiments.

(2) Agreement with MFT predictions: The MFT slip-size distribution depends on stress τ as $D(S,\tau) \sim S^{-\kappa} f_S(S(\tau_c-\tau)^{1/\sigma})$ where κ=1.5, σ=0.5, and $f_S(x)$ is an exponentially decaying universal scaling function [2]. Consequently the largest expected avalanche-size $S_{max}(\tau)$ grows with stress as $S_{max}(\tau) \sim (\tau_c-\tau)^{-1/\sigma}$. For the first time we extract and collapse the experimental avalanche-size distributions $D(S,\tau)$ from different stress-bins. The scaling-collapse agrees with the MFT predictions for κ=1.5, σ=0.5, and the scaling-*function*, which contains more information than the traditionally fitted power-law exponent κ alone. This collapse thus constitutes a much more stringent test of MFT, confirming that the slip statistics of plasticity indeed reflect the underlying *tuned non-equilibrium critical point* predicted by MFT [1-3], as explained above. The model also explains our observed dependence of the slip-statistics on compression rate and system size.

(3) Universality: The simple MFT provides a unified understanding of plasticity at nano- and micro-scales [10-12]. In experiments, at first sight, plasticity looks different on these two scales. At nano-scales the lattice structure matters. For example, the dislocation dynamics and the criticality-slope (defined as the slope of the stress-strain curve prior to failure (Figure 1C)), depend on the material's crystal structure [9-12,17]. Here, we show (a) how MFT relates these features to the slip-statistics, and (b) that MFT applies to all crystal structures on nano- and micro-scales, despite the apparent differences observed in experiments.

In summary, we show that MFT provides a unified explanation for plasticity as a tuned critical phenomenon under a wide variety of conditions: for pillar sizes ranging from 75 nm to 1 μm, for strain rates less than or on the order of $1x10^{-4}$ s^{-1}, for different materials and for different crystal structures. It predicts the power-law exponents and scaling function of the slip-size distributions, and the stress-dependence of their cutoffs.

In the following we first discuss the model predictions and then compare them to stress-integrated and stress-binned (i.e. stress-dependent) slip-size distributions measured during uniaxial compression of nano-pillars for different values of stress, deformation rate, and pillar-size. The analysis tools and methods [18] applied here to experiments are generally applicable to a much broader set of future experiments on plasticity and slip-avalanche statistics [19,20].

Simple MFT model for slow shear: Our simple coarse-grained model is described in detail in [2]. It makes robust statistical predictions for material deformation given the following assumptions:

1. A slowly sheared material has weak spots where slip initiates when the local stress exceeds a random local threshold stress.

2. Slip-avalanches occur at length scales that are large compared with the microscopic structure of the material.

3. The material is sheared sufficiently slowly so that slip-avalanches do not overlap in time.

4. The MFT approximation replaces the long-range elastic interactions with infinite range interactions.

A failed spot slips until the local stress is reduced to a random arrest stress, and then re-sticks. The stress released by a failed spot triggers other elastically coupled weak spots to slip, creating a slip-avalanche. According to assumption 3, avalanches occur faster than the slow, imposed material deformation. We extract detail-independent (universal) analytical predictions [2], which agree with numerical studies of continuum models [1,21], phase fields [22], phase field crystals [23], discrete 2D dislocation dynamics [1,3,21,24,25], and full 3D dislocation dynamics simulations [26].

At applied stress τ, the model predicts that the stress-dependent ("stress-binned") distribution $D(S, \tau)$ of slip-sizes S follows a power-law $S^{-\kappa}$ up to a stress-dependent cutoff size $S_{max} \sim (\tau_c-\tau)^{-1/\sigma}$ (this is the tuneability prediction of MFT) [2]:

$$D(S,\tau) \sim S^{-\kappa} f_S(S(\tau_c-\tau)^{1/\sigma}).$$

Here S is the total displacement during a slip-avalanche (see SOM). The exponents $\kappa=3/2$ and $1/\sigma=2$ and the cutoff scaling-function $f_S(x)$ are universal [1,2]. In MFT, $f_S(x) = \exp(-Ax)$ where A is a non-universal constant [2]. τ_c is again the failure-stress, also called "critical stress". The stress-binned complementary cumulative distribution-function (CCDF) is

$$C(S,\tau) \sim \int_S^{\infty} D(S',\tau)dS' \sim S^{-(\kappa-1)} g(S(\tau_c-\tau)^{1/\sigma}) \qquad (1)$$

where $g(x) \equiv \int_x^{\infty} e^{-At} t^{-\kappa} dt$ is the universal scaling-function (see Figure 4, inset). MFT predicts that the stress-integrated histogram $D_{int}(S)$ of slip-sizes follows a power-law (see SOM)

$$D_{\text{int}}(S) \equiv \int D(S,\tau)d\tau \sim S^{-(\kappa+\sigma)} \qquad (2)$$

with $\kappa+\sigma=2$. The stress-integrated CCDF

$$C(S) \equiv \int_S^{\infty} D_{\text{int}}(S')dS' \sim S^{-(\kappa+\sigma-1)} \qquad (3)$$

then scales as $C(S) \sim S^{-1}$ in MFT (Figures 2-4). MFT predicts identical power-law exponents for fcc nano-pillars (whose stress strain curves end with the virtually-vanishing criticality-slopes), as for bcc metals (with a finite, non-zero criticality-slope) [2,17]. The above predictions apply to slow compression rates where avalanches are separated in time.

At higher compression rates Ω, avalanches can overlap in time. A general theory [27] predicts that merging of avalanches in time, i.e. activating new avalanches before the previous ones complete, leads to smaller exponent values at higher Ω [27]: at faster compression rates Ω we expect $\kappa+\sigma<2$, while at slow Ω we expect $\kappa+\sigma=2$ (Figure 3 and Eq.(2)).

Compression experiments on single-crystalline nano-pillars: Experimental load and displacement data were obtained from uniaxial compressions of fcc and bcc single-crystalline, cylindrical nano-pillars with diameters ranging from 75 nm to 1000 nm and aspect ratios (height/diameter) between 3:1 and 6:1 (Figure 1). The experimental procedure (methods section) provided time series of applied load, axial displacement, and slip-sizes S for each tested pillar. The sampling frequency was 25 Hz, and by noting where the slip-distribution changes from power-law to Gaussian we concluded that slip identification was reliable down to events as small as O(0.3nm). Au, Nb, Mo, Ta, and W nano-pillars were fabricated via focused ion beam (FIB) methodology [9,15,16], and Cu pillars were created via templated electroplating [28], and were compressed at various displacement rates. For slowly increasing applied load, the stress remains approximately constant during each slip, as assumed in the model. This applies to all experiments, as the

slip speed is much greater than the externally imposed strain rates [29]. The data were collected on two nanoindenters, one with high stiffness of 300000 N/m, and one with stiffness of 65000 N/m; no systematic difference based on machine stiffness was observed.

Figures 2-4 and 5 respectively show experimental stress-integrated and stress-binned complementary cumulative histograms. The major source of error is statistical, caused by small event-numbers. Across all tested materials, the cumulative histograms display a power-law regime with an exponent close to the theoretical value of -1 (see Figure 2). The data in Figure 2 were collected for large system-sizes and at low nominal displacement rates − a regime closest to the scaling regime of the MFT model. These plots show that both fcc and bcc nano-crystals of different diameters and compressed at different displacement rates display the same power-law exponents despite the distinct differences in their dislocation behavior as reported in [9,17]. The materials show slight differences in how the changing nominal displacement rates affect the statistical data.

Figure 3 shows the results for three different nominal displacement rates, varying by an order of magnitude, for 800nm diameter Au and Mo pillars. The avalanche-size distribution for Mo is fairly robust from 0.1 to 1nm/s, but the magnitude of the fitted scaling exponent of *C(S)* decreases at 10nm/s. Au is much more sensitive to the prescribed displacement rate: the magnitude of the scaling exponent of *C(S)* again decreases with the increasing displacement rate. As discussed in the theory section and in [27], at higher driving rates avalanches can overlap in time, thereby reducing the scaling exponents of *C(S)*. Note that limited time resolution may also cause avalanches to appear as overlapping in time. Theory predicts that the amounts by which the exponents change as the displacement rate is increased depend on the material [27], as corroborated by our experiments. The results of Figure 3 for different nominal displacement rates are thus consistent with the theories of [2] and [27].

We also considered the impact of system-size on the slip-size distributions. Sufficiently close to the critical (failure) stress, the correlation length reaches the system-size. Consequently the pillar diameter projected onto a shear slip-plane determines the scale of the largest slip-events, and, hence, the cutoff of the stress-integrated slip-size distribution. Figure 4 shows *C(S)* for Cu, for various nano-pillar sizes compressed at the same displacement rate of 2nm/s. Although events are few and statistical fluctuations pronounced, the trend of increasing maximum avalanche-size with system-size is visible in Figure 4.

Figure 5 shows that the cumulative slip-size histograms binned in stress also agree with the model's prediction for $C(S,\tau)$ of Eq. (1) (see SOM). The main figure shows data from four distinct stress-bins, while the inset shows a data collapse using the exponents κ-1= 0.5 and $1/\sigma$=2 predicted by MFT. Stress-bins closer to the critical stress than those shown were not used in the collapse, in order to avoid finite size effects (since near the critical stress, the correlation-length is capped by the system-size, see SOM). The inset shows that the theoretically predicted collapse function (continuous grey line) falls on top of the experimental collapse. This reveals that MFT not only predicts the exponents used for the successful collapse, but also predicts the scaling-function [2]. This constitutes the first experimental validation of a universal scaling-function predicted by the simple MFT

model. The collapse also confirms the stress-integrated power-law of -1 for *C(S)* seen in Figures 2-4.

Discussion: Recent uniaxial deformation experiments and simulations provide insight into the physical nature of dislocation sources, size dependence of material strength, strain rate sensitivity, and amount of hardening [10-12]. The consensus is that these factors vary greatly between fcc and bcc crystals, and from nano- to microscale. The question emerges whether these differences are also manifested by the dislocation slip statistics. Our experiments yield a stress-integrated exponent of $\kappa+\sigma=2$ for the slip-size distributions, for both bcc and fcc nano-pillars with diameters between 75nm and 1μm, in agreement with the MFT prediction. In contrast, previous experiments on Mo and Au [9,14] have reported a size-distribution exponent of 1.5 for samples ranging in size from 180nm to 6μm. Our model provides a unified understanding of the statistics in all these cases:

(1) The compression experiments of [14] on sub-micron samples were performed at higher effective compression-rates (Figure 3), where lower exponents can be explained by the merging, of slip-avalanches [27]. We observed significant impact on the exponent for rates as slow as 1nm/s.

(2) Many micron-sized samples display a large regime before failure where the stress-strain curve is linear due to hardening [8,11]. Such behavior can be captured by modifying the MFT model to include hardening through incorporating an increased resistance to slip during deformation. In this case, the effective stress-distance from criticality remains constant [1], and the experiment effectively measures κ rather than $\kappa+\sigma$. In this case the SOC assumption [5,6,8] with the measured value of $\kappa=1.5$ is valid and agrees with the MFT predictions [1, 2, 26, 30].

In conclusion, this study presents the first scaling-collapse and scaling-function extracted from compression experiments on nanopillars and micropillars. It shows that plasticity is a *tuned* critical phenomenon. Both the exponents and the scaling-function of the stress-dependent strain-bursts statistics agree with predictions from a simple analytical MFT model. This agreement constitutes the most stringent test of the MFT model and tuned criticality to date, since scaling-functions contain much more information than the traditional sets of exponents. The agreement between the MFT model and experiments for a wide variety of metallic nano-crystals subjected to widely varying experimental conditions suggests that a single universality class fully describes discrete crystalline deformation at these small length scales. This holds true under a wide variety of conditions: for pillar sizes ranging from 75 nm to 1 μm, for strain rates less than or on the order of 1×10^{-4} s^{-1} and for different materials including those with fcc and bcc crystal structures. This agreement is observed both in the power-law scaling of the event frequency as well as in the stress-dependence of the slip-size distributions. This robustness indicates that these analysis methods are broadly applicable to other non-equilibrium systems with driving-force dependent avalanches [19]. In the context of the renormalization group [2,18,19] our results imply that the same fundamental properties—

symmetries, dimensions, interaction range, etc.—control the statistics of slips in metallic crystals, down to the smallest currently accessible length scales.

Acknowledgements: We thank James Antonaglia, Braden Brinkman, Dennis Dimiduk, Tyler Earnest, Robert Maass, Molei Tao, and Matthew Wraith for helpful conversations and acknowledge the financial support of a NSERC Post-Graduate Scholarship (NF), and from grants NSF DMR 03-25939 ITR ("Materials Computation Center") and DMR 1005209 (GT and KD), as well as from NSF Graduate Fellowship (ATJ), NSF CAREER award DMR-0748267 (JRG) and ONR Grant No. N00014-09-1-0883 (JRG). KD also thanks the Kavli Institute of Theoretical Physics at UC Santa Barbara for hospitality and support.

References

[1] Zaiser, M., Scale invariance in plastic flow of crystalline solids, *Advances in Physics* **55**, 185-245 (2006).

[2] Dahmen, K.A., Ben-Zion, Y. & Uhl, J.T., A micromechanical model for deformation in solids with universal predictions for stress-strain curves and slip-avalanches, *Phys. Rev. Lett.* **102**, 175501/1-4 (2009).

[3] Miguel, M.-C., Vespignani, A., Zapperi, S., Weiss, J. & Grasso, J.R., Intermittent dislocation flow in viscoplastic deformation, *Nature* **410**, 667-671 (2001).

[4] Weiss, J., Grasso, J.R., Miguel, M.-C., Vespignani, A. & Zapperi, S., Complexity in dislocation dynamics: experiments, *Mater. Sci. Eng. A* **309-310**, 360-364 (2001).

[5] Richeton, T., Dobron, P., Chmelik, F., Weiss, J. & Louchet, F., On the critical character of plasticity in metallic single crystals, *Mater. Sci. Eng. A* **424**, 190-195 (2006).

[6] Richeton, T., Weiss, J. & Louchet, F., Dislocation avalanches: Role of temperature, grain size and strain hardening, *Acta Materialia* **53**, 4463-4471 (2005).

[7] Weiss, J., Lahaie, F. & Grasso, J.R., Statistical analysis of dislocation dynamics during viscoplastic deformation from acoustic emission, *J. Geo. Res*. **105**, 433-442 (2000).

[8] Dimiduk, D.M., Woodward, C., LeSar, R. & Uchic, M.D., Scale-free intermittent flow in crystal plasticity, *Science* **312**, 1188-1190 (2006).

[9] Brinckmann, S., Kim, J.-Y. & Greer, J.R., Fundamental differences in mechanical behavior between two types of crystals at the nanoscale, *Phys. Rev. Lett.* **100**, 155502/1-4 (2008).

[10] Greer, J.R. & De Hosson, J.T.M**.,** Plasticity in small-sized metallic systems: intrinsic versus extrinsic size effect, *Progress in Materials Science* **56**, 654-724 (2011).

[11] Uchic, M.D., Shade, P. & Dimiduk, D., Plasticity of micrometer-scale single crystals in compression, *Annual review of materials research* **39**, 361-386 (2009) and references therein.

[12] Kraft, O., Gruber, P., Mönig, R. & Weygand, D., Plasticity in confined dimensions, *Annual review of materials research* **40**, 293-317 (2010) and references therein.

[13] Ngan, A.H.W. & Ng, K.S., Transition from deterministic to stochastic deformation, *Phil. Mag.* **90**, 1937-1954 (2010).

[14] Zaiser, M., Schwerdtfeger, J., Schneider, A.S., Frick, C.P., Clark, B.G., Gruber, P.A. & Arzt, E., Strain bursts in plastically deforming molybdenum micro- and nanopillars, *Phil. Mag.* **88**, 3861 – 3874 (2008).

[15] Kim, J.-Y. & Greer, J.R., Tensile and compressive behavior of gold and molybdenum single crystals at the nano-scale, *Acta Materialia* **57**, 5245 – 5253 (2009).

[16] Kim, J.-Y., Jang, D. & Greer, J.R., Tensile and compressive behavior of tungsten, molybdenum, tantalum and niobium at the nanoscale, *Acta Materialia* **58**, 2355 – 2363 (2010).

[17] Weinberger, C.R. & Cai, W., Surface-controlled dislocation multiplication in metal micropillars, *Proceedings of the National Academy of Sciences of the United States of America* **105**, 14304-14307 (2008).

[18] Goldenfeld, N.D., *Lectures on Phase Transitions and the Renormalization Group.* Westview Press (1992).

[19] Sethna, J.P., Dahmen, K.A. & Myers, C.R., Crackling noise, *Nature* **410**, 242-250 (2001).

[20] Mehta, A.P., Mills, A.C., Dahmen, K.A. & Sethna, J.P., Universal pulse shape scaling function and exponents: Critical test for avalanche models applied to Barkhausen noise, *Physical Review E* **65**, 046139/1-6 (2002).

[21] Zaiser, M., The 'yielding transition' in crystal plasticity - discrete dislocations and continuum models, *Statistical Mechanics of Plasticity and Related Instabilities*, provided by the SAO/NASA Astrophysics Data System (2005).

[22] Koslowski, M., Scaling laws in plastic deformation, *Phil. Mag.* **87,** 1175-1184 (2007).

[23] Chan, P.Y., Tsekenis, G., Dantzig, J., Dahmen, K.A. & Goldenfeld, N., Plasticity and dislocation dynamics in a phase field crystal model, *Phys. Rev. Lett*. **105**, 015502/1-4 (2010).

[24] Tsekenis, G., Goldenfeld, N. & Dahmen, K.A., Dislocations jam at any density, *Phys. Rev. Lett.* **106**, 105501/1-4 (2011).

[25] Ispanovity, P.D., Groma, I., Gyorgyi, G., Csikor, F.F. & Weygand, D., Submicron plasticity: Yield stress, dislocation avalanches, and velocity distribution, *Phys. Rev. Lett.* **105**, 085503/1-4 (2010).

[26] Csikor, F.F., Motz, C., Weygand, D., Zaiser, M. & Zapperi, S., Dislocation avalanches, strain bursts, and the problem of plastic forming at the micrometer scale, Science **318**, 251-254 (2007).

[27] White, R.A. & Dahmen, K.A., Driving rate effects on crackling noise, *Phys. Rev. Lett*. **91**, 085702/1-4 (2003).

[28] Jennings, A.T., Burek, M.J. & Greer, J.R., Microstructure versus size: Mechanical properties of electroplated single crystalline Cu nanopillars, *Phys. Rev. Lett.* **104**, 135503/1-4 (2010).

[29] Jennings, A.T., Li, J. & Greer, J.R., Emergence of strain rate sensitivity in Cu nanopillars: Transition from dislocation multiplication to dislocation nucleation, *Acta Mat.* **59**, 5627-5637 (2011).

[30] Tsekenis, G., Uhl, J.T., Goldenfeld, N. & Dahmen, K.A., Temporal and finite size scaling properties of avalanches in plasticity exhibit mean field character, submitted to *Phys. Rev. B* (2012).

[31] Newman, M.E.J., Power laws, Pareto Distributions and Zipf's law, *Contemporary Physics* **46**, 323-351 (2005).

Figures

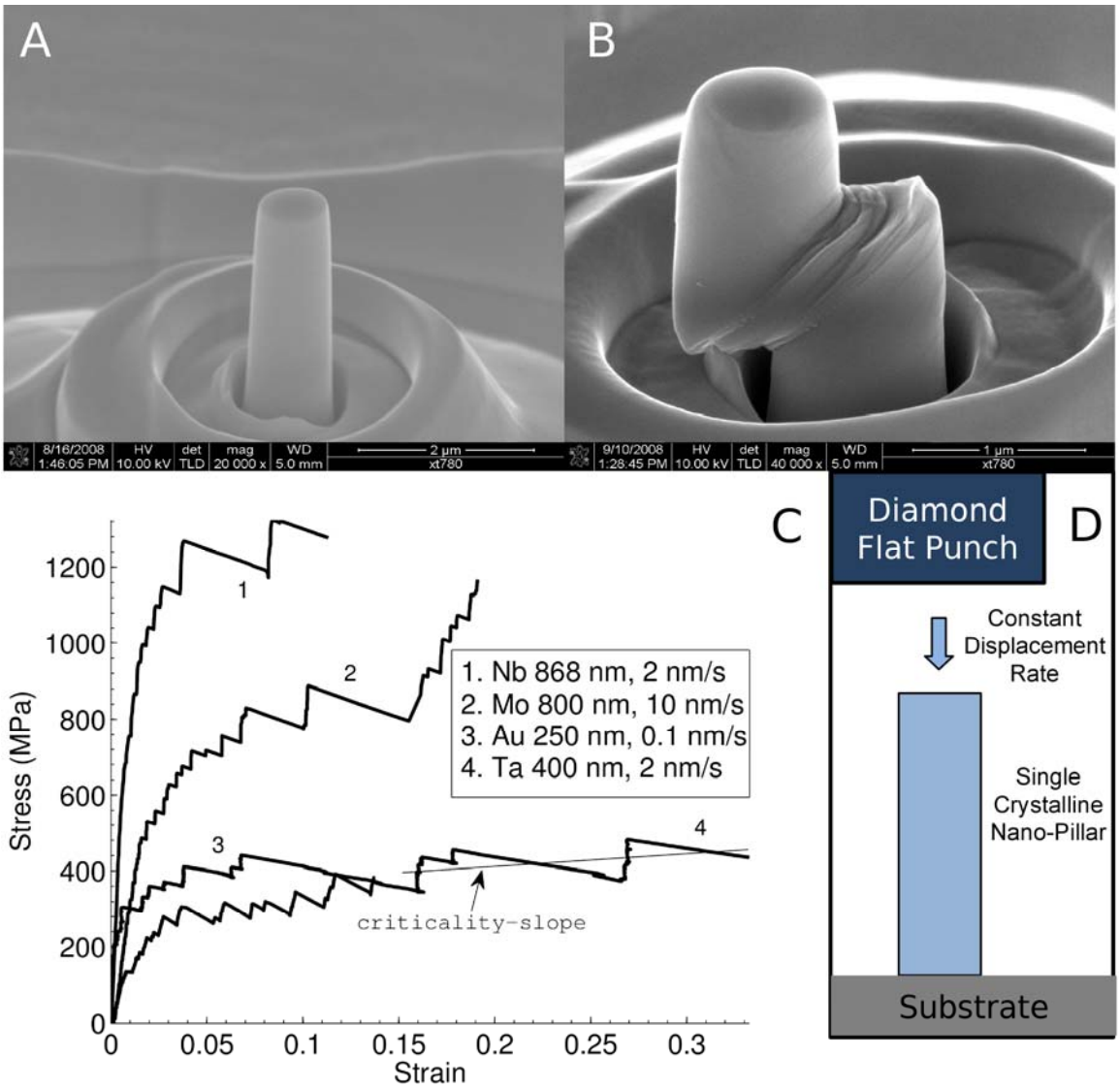

Figure 1: Nano-pillar compression tests. A,B: SEM images of a 868nm-diameter Nb pillar at 52º tilt, before and after compression, respectively. B: Pillar after final catastrophic slip-event; slip-data at the largest strains is excluded from the analysis. C: Characteristic stress-strain curves (each contains thousands of points) for four metals compressed at different displacement-rates. Negatively-sloped lines connect two points at beginning and end of fast slips, with spring-like machine-response. The Nb stress-strain curve corresponds to the pillar in A-B. The "criticality-slope" line is fitted to the average slope of curve 4, near the critical (failure) stress (see text). D: schematic of the compression test methodology. For details see SOM.

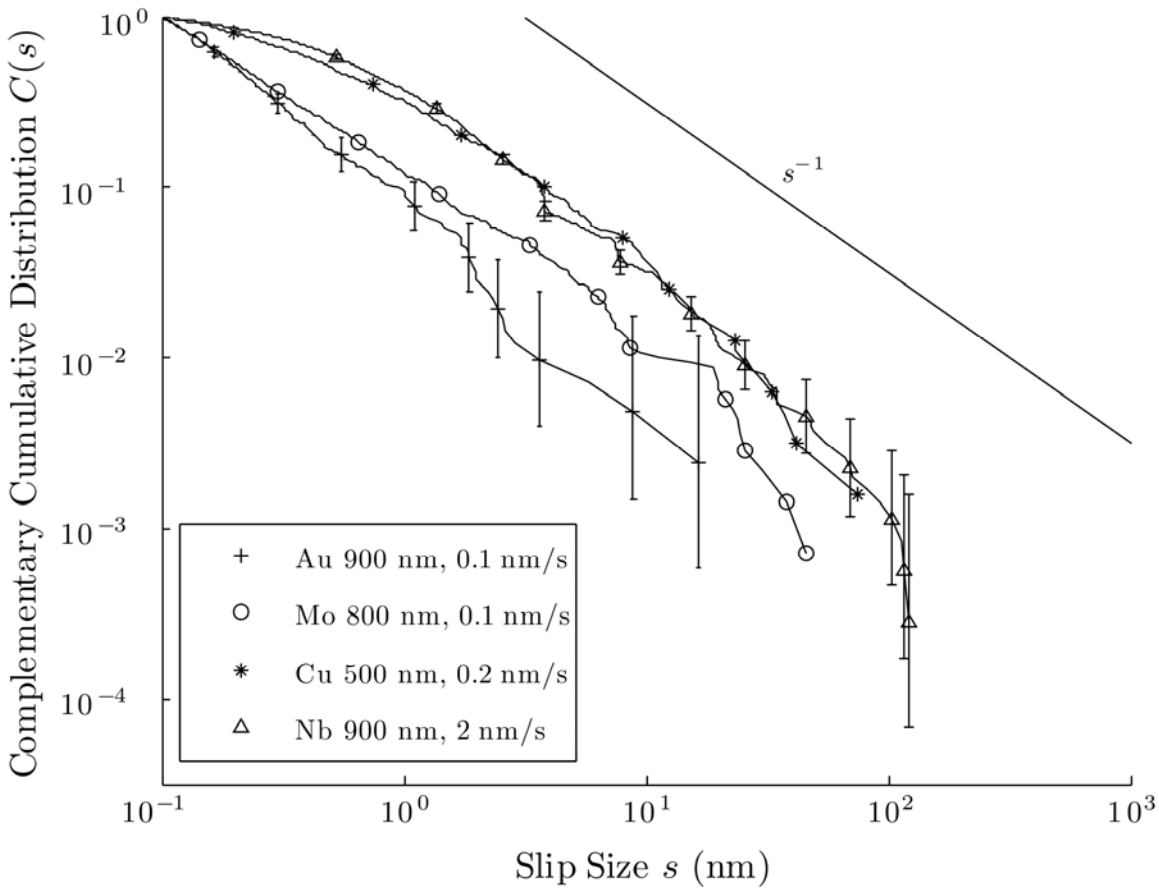

Figure 2: Stress-integrated cumulative histograms *C(S)* of slip-sizes *S* (i.e. the fraction of slips with sizes > *S* plotted versus *S*) for uniaxial compression of various materials, pillar-sizes, and nominal displacement-rates, integrated over stress from zero to critical (failure) stress. *C(S)* contains hundreds of points (one point per event). Error-bars (from Bayesian 95% confidence bounds (see SOM)) are shown for histograms with the most and the least points for clarity. Fitted PDF power-law exponents: 2.1±0.1 (Au), 1.85±0.1 (Mo), 1.8±0.2 (Cu), and 1.9±0.2 (Nb) (subtract 1 for CDF exponents). Fits were obtained from maximum likelihood estimates [31] (see SOM for error bars and fitting techniques for all figures).

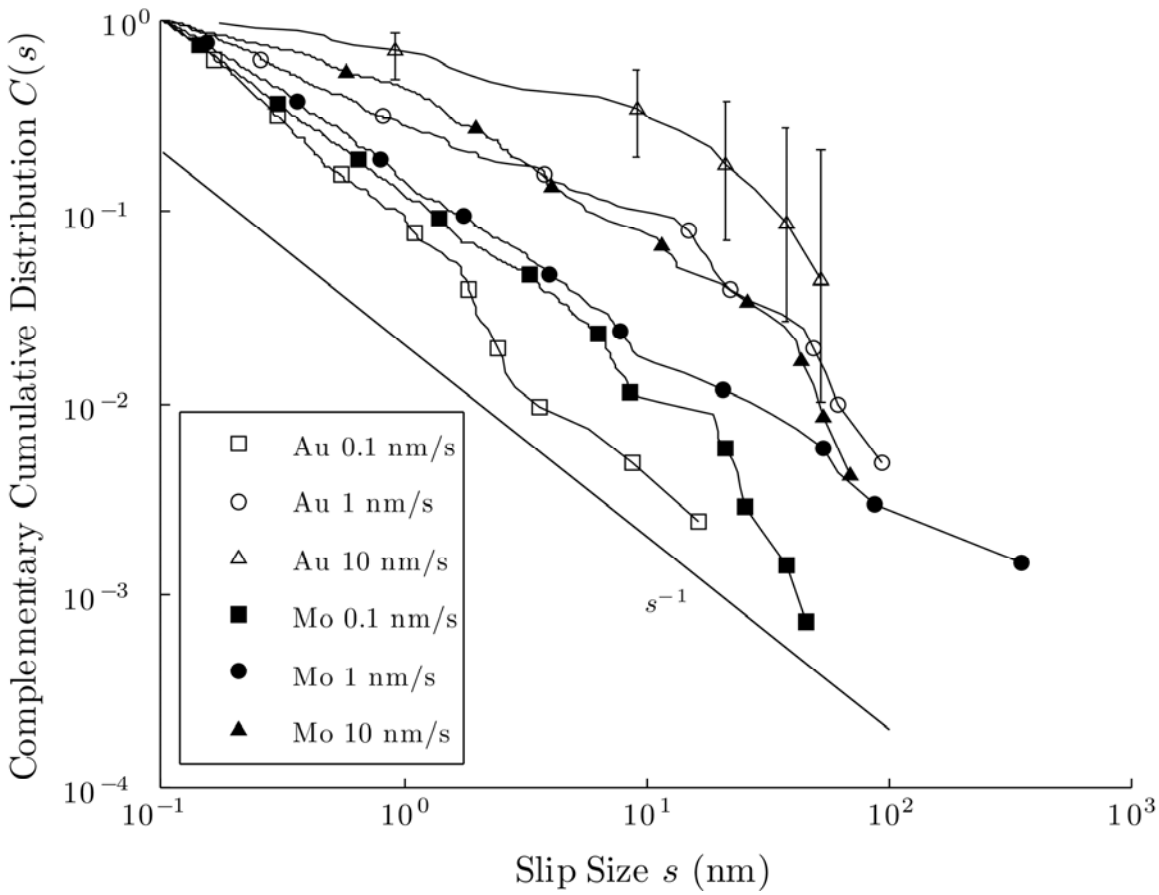

Figure 3: Stress-integrated cumulative histograms *C(S)* of slip-sizes *S* for uniaxial compression data: comparison of the impact of nominal displacement-rate for Mo and Au pillars of diameter 800nm. The nominal displacement-rate impacts the apparent power-laws of the cumulative slip-size histograms. The fitted PDF exponents are: 2.1±0.1, 1.45±0.1, 1.2±0.2, 1.85±0.1, 1.8±0.1, and 1.6±0.3, in the order of the legend (subtract 1 for CDF exponents). The lowest rates are used to compare with model predictions.

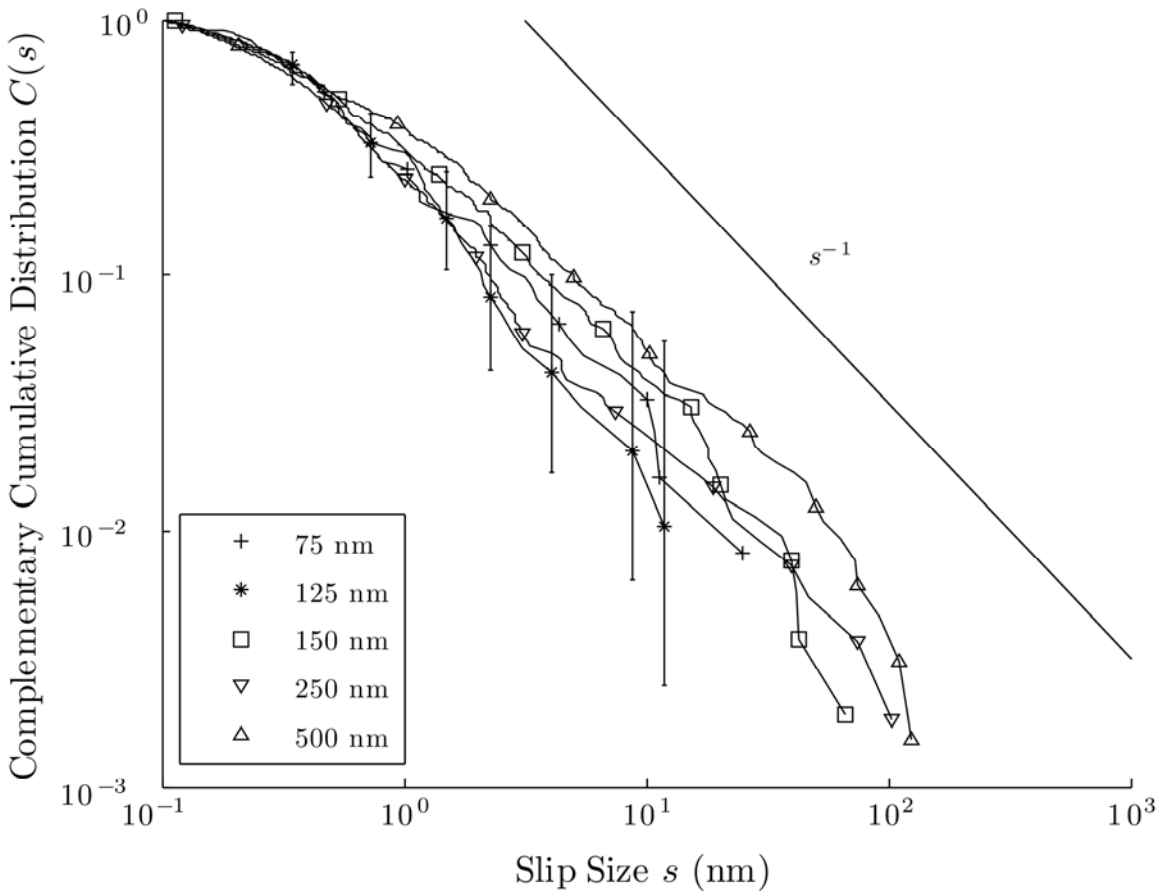

Figure 4: Stress-integrated cumulative histograms *C(S)* of the slip-size *S* for various sizes of Cu nano-pillars compressed at a displacement-rate of 2 nm/s. Larger pillars have larger maximum slip-events, except for the 125nm pillars, for which less data was taken. (For power-law distributions, the largest expected slip-size increases with the total number of slips.)

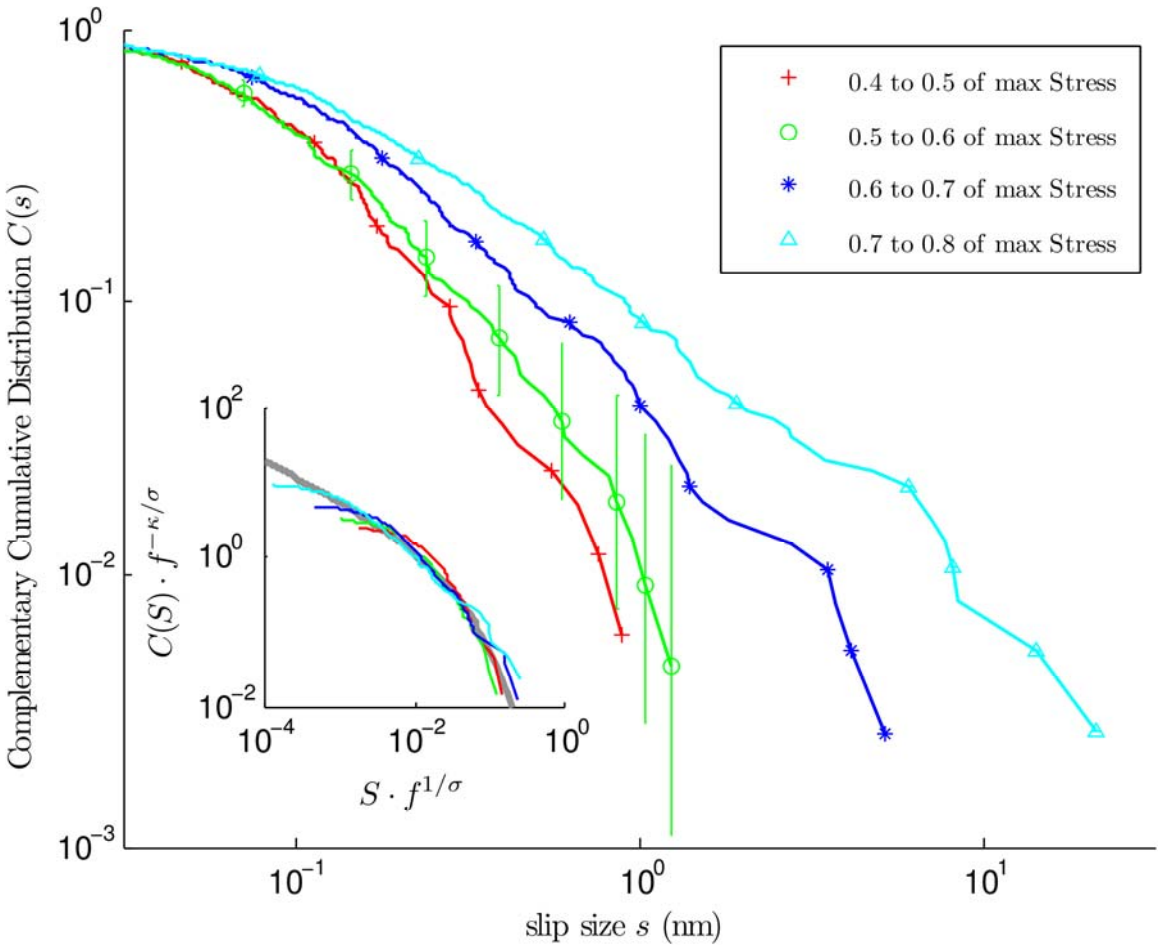

Figure 5: **Main figure**: Stress-binned cumulative histogram *C(S,τ)* of slip-sizes *S* as a function of applied stress τ, using events from 7 Mo nano-pillars, of approximate diameter 800nm, compressed at 0.1nm/s nominal displacement rate. The events from each pillar are normalized according to their respective maximum stress. **Inset**: Scaling-collapse of the same data, $f = (\tau_c - \tau)/\tau_c - c'$, where $c' = 0.14$ is an adjustable parameter that compensates for finite system-size (see SOM); $\kappa = 1.5$ and $1/\sigma = 2$ (as predicted by MFT), the grey function is the predicted MFT scaling-function, $g(x) \equiv \int_x^\infty e^{-At} t^{-\kappa} dt$.